

## 8 Problem VDPOL

### 8.1 General information

The problem consists of a second order differential equation rewritten to first order form, thus providing a system of ordinary differential equations of dimension 2. It was proposed by B. van der Pol in the 1920's [vdP20], [vdP26]. The INdAM-Bari Test Set group contributed this problem to the test set. Most of the documentation about this problem has been retrieved from [EP02]. The software part of the problem is in the files `vdpol.f` and `vdpolm.f` available at [MM08].

### 8.2 Mathematical description of the problem

The problem is of the form

$$z'' = f(z, z'), \quad z(0) = z_0 \quad z'(0) = z'_0,$$

with

$$z \in \mathbb{R}, \quad t \in [0, T],$$

where the function  $f$  is given by

$$f(z, z') = \mu(1 - z^2)z' - z, \quad \mu > 0. \quad (\text{II.8.1})$$

We write this problem to first order form by defining  $y_1 = z$  and  $y_2 = z'$ , yielding a system of 2 nonlinear differential equations of the form

$$\begin{pmatrix} y_1 \\ y_2 \end{pmatrix}' = \begin{pmatrix} y_2 \\ f(y_1, y_2) \end{pmatrix} \quad (\text{II.8.2})$$

with

$$(y_1, y_2)^T \in \mathbb{R}^2, \quad t \in [0, T].$$

A rescaling of the solutions of (II.8.2) results in the following formulation

$$\begin{pmatrix} y_1 \\ y_2 \end{pmatrix}' = \begin{pmatrix} y_2 \\ \tilde{f}(y_1, y_2) \end{pmatrix}, \quad (\text{II.8.3})$$

where

$$\tilde{f}(y_1, y_2) = ((1 - y_1^2)y_2 - y_1)/\epsilon, \quad \epsilon > 0.$$

Problem (II.8.2) will be referred to as  $\text{vdpol}_\mu$  and problem (II.8.3) as  $\text{vdpol}_\epsilon$ . The initial values are

$$\begin{pmatrix} y_1(0) \\ y_2(0) \end{pmatrix} = \begin{pmatrix} z_0 \\ z'_0 \end{pmatrix} \quad \text{where} \quad \begin{cases} z_0 = 2 \\ z'_0 = 0 \end{cases}.$$

### 8.3 Origin of the problem

The VDPOL problem originates from electronics and describes the behaviour of nonlinear vacuum tube circuits. The circuit scheme, designed by Balthazar van der Pol in the 1920's, is given in Figure II.8.1. This is an RLC loop, but with the passive resistor of Ohm's Law replaced by an active element which would pump energy into the circuit whenever the amplitude of the current falls below a certain level. In the 1920's this active element was an array of vacuum tubes, now it is a semiconductor device. The voltage drop at the semiconductor (which used to be RI) is given by a nonlinear function  $f(I)$  of

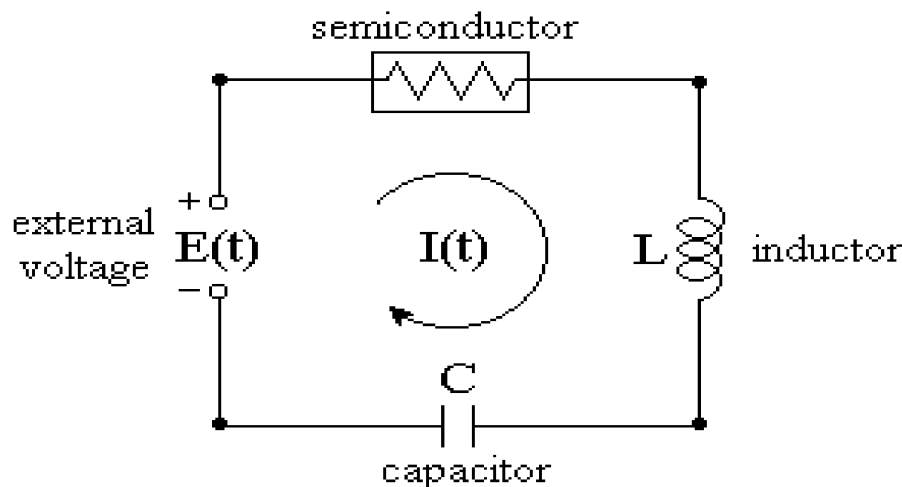


FIGURE II.8.1: Negative resistance oscillatory circuit

the current  $I$ . If we substitute  $f(I)$  for  $RI$  in the standard RLC-circuit equation  $LI'' + RI' + I/C = 0$ , the current in the circuit turns out to be modeled by

$$LI'' + f'(I)I' + I/C = 0. \quad (\text{II.8.4})$$

In a 1924 study of oscillator circuits in early commercial radios (at Philips research laboratories), B. van der Pol assumed the voltage drop to be represented by the nonlinear function  $f(I) = bI^3 - aI$ , which with equation (II.8.4) leads to

$$LI'' + (3bI^2 - a)I' + I/C = 0. \quad (\text{II.8.5})$$

This equation is also closely related to the equation introduced by the British mathematical physicist Lord Rayleigh (John William Strutt, 1842 - 1919) to model the oscillations of a clarinet reed. For more details see [EP02].

If we denote by  $\tau$  the time variable in Eq. (II.8.5) and make the substitutions  $I = pz$  and  $t = \tau/\sqrt{LC}$ , the result is

$$\frac{d^2z}{dt^2} + (3bp^2z^2 - a)\sqrt{\frac{C}{L}} \frac{dz}{dt} + z = 0.$$

With  $p = \sqrt{a/(3b)}$  and  $\mu = a\sqrt{C/L}$  this gives the standard form

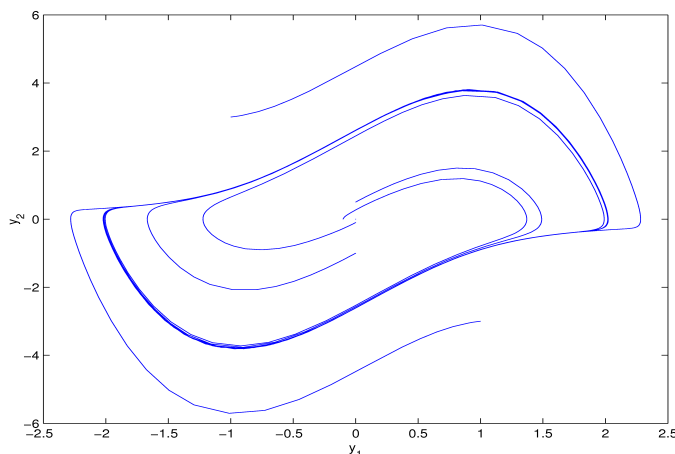
$$z'' + \mu(z^2 - 1)z' + z = 0$$

of the *van der Pol's equation*.

The van der Pol equation is often used as a test problem for ODEs solvers. It has two periodic solutions, the constant solution,  $z(t) \equiv 0$ , that is unstable, and the nontrivial periodic solution (roughly corresponding to the initial conditions  $z(0) = 2$ ,  $z'(0) = 0$ ), that is named 'limit cycle' because all the other nontrivial solutions converge to this one as  $t \rightarrow \infty$ .

This qualitative behavior is well shown in the phase plane plot in Figure II.8.2 (for  $\mu = 2$ ), where outward and inward spiral trajectories converge to the limit cycle (the closed curve).

The parameter  $\mu > 0$  weights the importance of the nonlinear part of the equation. When  $\mu$  is 'large' the approach to the limit cycle is quite rapid (see Figure II.8.3 for  $\mu = 10^3$ ) and the van der Pol equation is more interesting because of the non negligible influence of the nonlinear term. From

FIGURE II.8.2: *Limit cycle for  $\mu = 2$* 

an analysis of the behavior of the limit cycle [Sha94] it turns out that it can be described in terms of portions where the solution components change slowly and the problem is quite stiff, alternating with regions of very sharp change (quasi-discontinuities) where it is non-stiff. Thus, the problem switches from stiff to non stiff with a very sharp changing solution that makes the equation quite challenging for ODEs solvers.

The van der Pol equation may be treated in different ways, the most straightforward is to split the equation into a system of two first order differential equations as in (II.8.2). Note that if the second of the equations is divided by  $\mu$  we get an equation that has the character of a singular perturbation problem. Several other approaches may show other aspects on the nature of this problem. For example Hairer and Wanner [HW96] introduce the following scaling transformation of (II.8.2) to make the steady-state approximation independent of  $\mu$ :

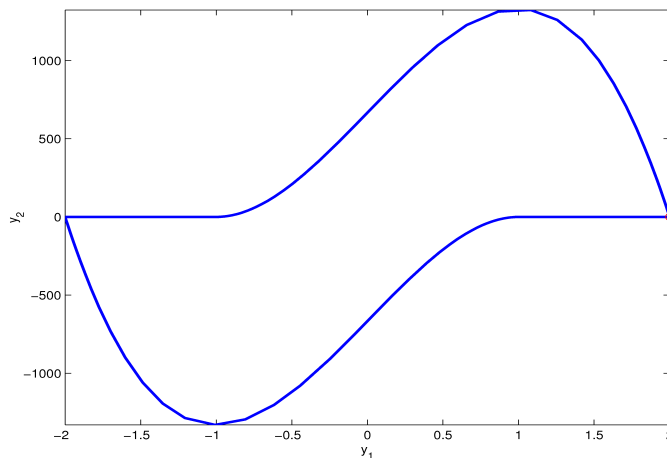
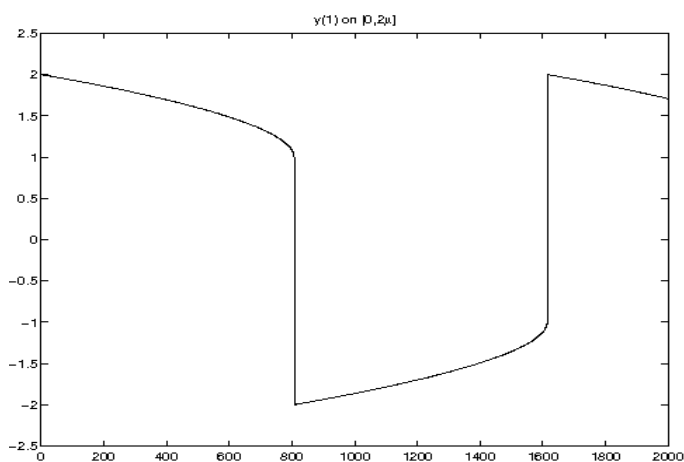
$$x = t/\mu, \quad w_1(x) = y_1(t), \quad w_2(x) = \mu y_2(t)$$

Substituting in (II.8.2) and using again  $y$  for  $w$  and  $t$  for  $x$ , the equation (II.8.3) is obtained with  $\varepsilon = 1/\mu^2$ . The scaled version (II.8.3) has the advantage that a small interval independent of the parameter value can be considered to track at least one period of the solution.

## 8.4 Numerical solution of the problem

### 8.4.1 $\text{vdpol}_\mu$ with $\mu = 10^3$ and $t \in [0, 2\mu]$

Tables II.8.1, II.8.2 and Figures II.8.4, II.8.6–II.8.9 present the reference solution at the end of the integration interval, the run characteristics, the behavior of the first component of the solution over the integration interval and the work-precision diagrams, respectively. The reference solution was computed by RADAU on an Alphaserver DS20E, with a 667 MHz EV67 processor, using double precision `work(1) = uround = 1.01 · 10-19`, `rtol = atol = h0 = 1.1 · 10-18`. For the work-precision diagrams, we used: `rtol = 10-(4+m/4)`,  $m = 0, 1, \dots, 32$ ; `atol = rtol`; `h0 = 10-2 · rtol` for BIMD, GAMD, MEBDFDAE, MEBDFI, RADAU and RADAU5.

FIGURE II.8.3: *Limit cycle for  $\mu = 10^3$* FIGURE II.8.4: *Behavior of the solution component  $y_1$  over the integration interval*

#### 8.4.2 $\text{vdpol}_\epsilon$ with $\epsilon = 10^{-6}$ and $t \in [0, 2]$

Tables II.8.3, II.8.4 and Figures II.8.5, II.8.10–II.8.13 present the reference solution at the end of the integration interval, the run characteristics, the behavior of the first component of the solution over the integration interval and the work-precision diagrams, respectively. The reference solution was computed by RADAU on an Alphaserver DS20E, with a 667 MHz EV67 processor, using double precision  $\text{work}(1) = \text{uround} = 1.01 \cdot 10^{-19}$ ,  $\text{rtol} = \text{atol} = \text{h0} = 1.1 \cdot 10^{-18}$ . For the work-precision

TABLE II.8.1: *Reference solution at the end of the integration interval.*

$y_1$	$0.1706167732170469 \cdot 10^1$
$y_2$	$-0.8928097010248125 \cdot 10^{-3}$

TABLE II.8.2: *Run characteristics.*

solver	rtol	atol	h0	mescd	scd	steps	accept	#f	#Jac	#LU	CPU
BIMD	$10^{-4}$	$10^{-4}$	$10^{-6}$	4.05	3.57	133	112	2801	104	133	0.0020
	$10^{-7}$	$10^{-7}$	$10^{-9}$	9.18	8.80	224	219	5072	209	224	0.0029
	$10^{-10}$	$10^{-10}$	$10^{-12}$	11.17	10.32	250	248	10151	237	250	0.0078
DDASSL	$10^{-4}$	$10^{-4}$		2.88	2.37	549	507	940	122		0.0020
	$10^{-7}$	$10^{-7}$		5.57	5.06	1342	1296	1980	129		0.0049
	$10^{-10}$	$10^{-10}$		8.25	7.73	4484	4445	5943	168		0.0166
GAMD	$10^{-4}$	$10^{-4}$	$10^{-6}$	4.86	4.30	129	90	5133	91	129	0.0039
	$10^{-7}$	$10^{-7}$	$10^{-9}$	7.55	6.71	173	137	9422	141	173	0.0078
	$10^{-10}$	$10^{-10}$	$10^{-12}$	9.53	9.17	235	197	16067	201	235	0.0127
MEBDFI	$10^{-4}$	$10^{-4}$	$10^{-6}$	3.31	2.86	477	435	1761	83	83	0.0029
	$10^{-7}$	$10^{-7}$	$10^{-9}$	6.11	5.60	1134	1083	3818	118	118	0.0059
	$10^{-10}$	$10^{-10}$	$10^{-12}$	9.06	8.55	2135	2098	7215	208	208	0.0107
PSIDE-1	$10^{-4}$	$10^{-4}$		6.42	3.43	181	149	2811	57	648	0.0029
	$10^{-7}$	$10^{-7}$		7.20	6.32	310	293	6141	52	756	0.0059
	$10^{-10}$	$10^{-10}$		9.99	9.14	1000	990	15536	109	1156	0.0156
RADAU	$10^{-4}$	$10^{-4}$	$10^{-6}$	4.48	4.28	210	172	1822	144	208	0.0010
	$10^{-7}$	$10^{-7}$	$10^{-9}$	8.56	8.18	240	222	3508	187	238	0.0020
	$10^{-10}$	$10^{-10}$	$10^{-12}$	10.63	9.24	209	176	6240	130	207	0.0039
VODE	$10^{-4}$	$10^{-4}$		3.29	3.08	545	487	779	19	117	0.0020
	$10^{-7}$	$10^{-7}$		5.20	4.73	1614	1502	2145	30	223	0.0049
	$10^{-10}$	$10^{-10}$		7.49	7.07	4350	4120	5266	72	516	0.0146

diagrams, we used:  $\text{rtol} = 10^{-(4+m/4)}$ ,  $m = 0, 1, \dots, 32$ ;  $\text{atol} = \text{rtol}$ ;  $\text{h0} = 10^{-2} \cdot \text{rtol}$  for GAMD, MEBDFDAE, MEBDFI, RADAU and RADAU5.

TABLE II.8.3: *Reference solution at the end of the integration interval.*

$y_1$	$0.1706167732170483 \cdot 10^1$
$y_2$	$-0.8928097010247975 \cdot 10^0$

## References

- [EP02] C. H. Edwards and D. E. Penney. *Differential Equations and Linear Algebra*. Prentice Hall, 2002.
- [HW96] E. Hairer and G. Wanner. *Solving Ordinary Differential Equations II: Stiff and Differential-algebraic Problems*. Springer-Verlag, second revised edition, 1996.
- [MM08] F. Mazzia and C. Magherini. *Test Set for Initial Value Problem Solvers, release 2.4*. Department of Mathematics, University of Bari and INdAM, Research Unit of Bari, February 2008. Available at <http://www.dm.uniba.it/~testset>.

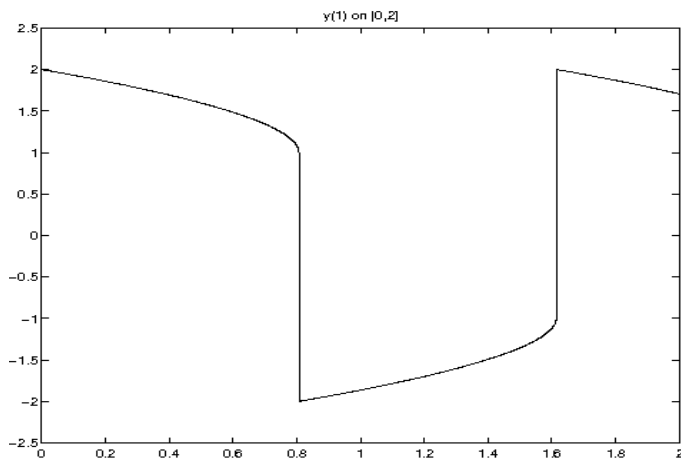
FIGURE II.8.5: Behavior of the solution component  $y_1$  over the integration interval (scaled equation)

TABLE II.8.4: Run characteristics.

solver	rtol	atol	h0	mescd	scd	steps	accept	#f	#Jac	#LU	CPU
BIMD	$10^{-4}$	$10^{-4}$	$10^{-6}$	4.31	3.98	170	155	3684	151	170	0.0029
	$10^{-7}$	$10^{-7}$	$10^{-9}$	9.06	8.73	301	293	7631	280	301	0.0059
	$10^{-10}$	$10^{-10}$	$10^{-12}$	11.17	10.84	307	304	13339	292	307	0.0088
DDASSL	$10^{-4}$	$10^{-4}$		2.89	2.56	796	776	1260	127		0.0029
	$10^{-7}$	$10^{-7}$		5.89	5.57	1943	1912	2796	149		0.0078
	$10^{-10}$	$10^{-10}$		8.96	8.64	6166	6110	7973	223		0.0234
GAMD	$10^{-4}$	$10^{-4}$	$10^{-6}$	5.40	5.08	148	105	6999	105	148	0.0049
	$10^{-7}$	$10^{-7}$	$10^{-9}$	6.52	6.19	163	133	12727	131	163	0.0098
	$10^{-10}$	$10^{-10}$	$10^{-12}$	10.16	9.84	244	216	18095	215	244	0.0137
MEBDFI	$10^{-4}$	$10^{-4}$	$10^{-6}$	3.86	3.53	638	591	2179	92	92	0.0029
	$10^{-7}$	$10^{-7}$	$10^{-9}$	6.99	6.67	1369	1317	4735	132	132	0.0078
	$10^{-10}$	$10^{-10}$	$10^{-12}$	10.80	10.47	2862	2858	9489	287	287	0.0146
PSIDE-1	$10^{-4}$	$10^{-4}$		5.70	5.38	235	166	4402	73	780	0.0049
	$10^{-7}$	$10^{-7}$		8.72	8.39	414	386	7896	75	908	0.0078
	$10^{-10}$	$10^{-10}$		11.40	11.07	1388	1365	23066	131	1360	0.0224
RADAU	$10^{-4}$	$10^{-4}$	$10^{-6}$	4.77	4.44	242	207	2214	165	231	0.0020
	$10^{-7}$	$10^{-7}$	$10^{-9}$	8.28	7.95	186	149	5212	102	173	0.0029
	$10^{-10}$	$10^{-10}$	$10^{-12}$	11.47	11.14	245	215	7589	148	224	0.0049
VODE	$10^{-4}$	$10^{-4}$		2.93	2.61	788	702	1186	21	181	0.0029
	$10^{-7}$	$10^{-7}$		5.65	5.32	2375	2200	3091	41	345	0.0088
	$10^{-10}$	$10^{-10}$		8.42	8.09	6426	6058	7814	106	794	0.0215

[Sha94] Lawrence F. Shampine. *Numerical solution of ordinary differential equations*. Chapman & Hall, New York, 1994.

[vdP20] B. van der Pol. *Radio Rev.*, 1:704–754, 1920.

[vdP26] B. van der Pol. On relaxation oscillations. *Phil. Mag.*, 2:978–992, 1926. reproduced in: B.

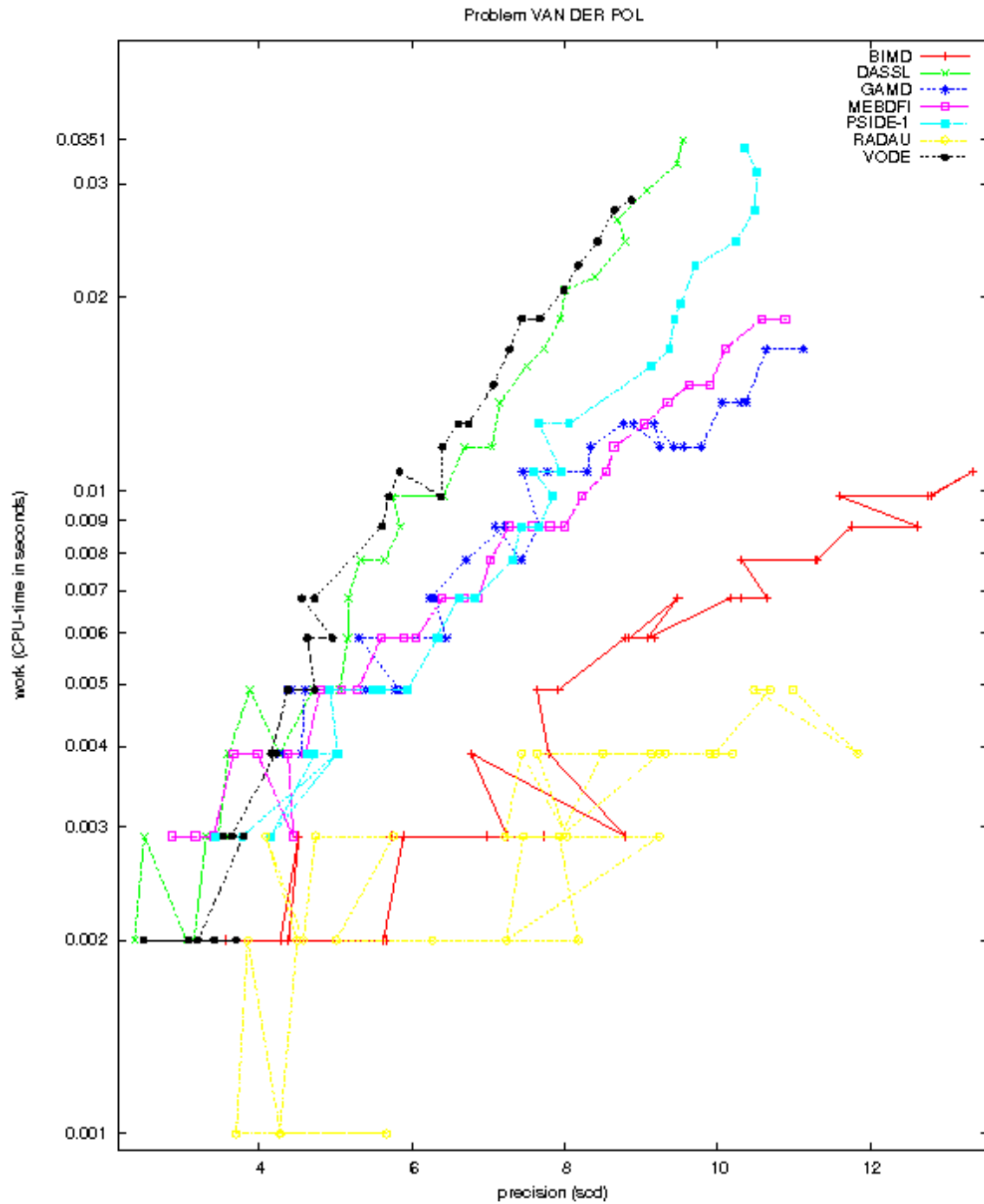


FIGURE II.8.6: Work-precision diagram (scd versus CPU-time).

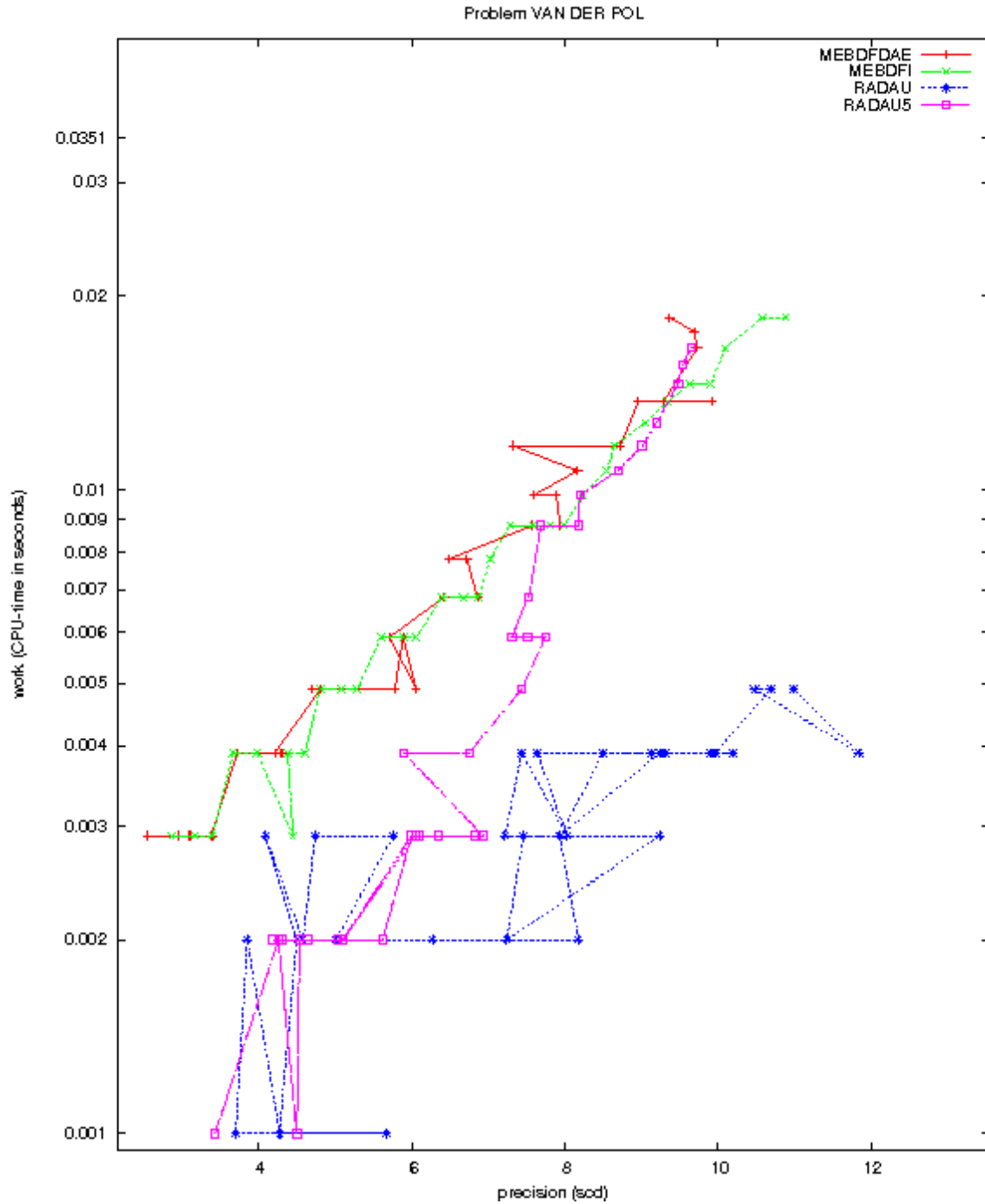


FIGURE II.8.7: Work-precision diagram (scd versus CPU-time).



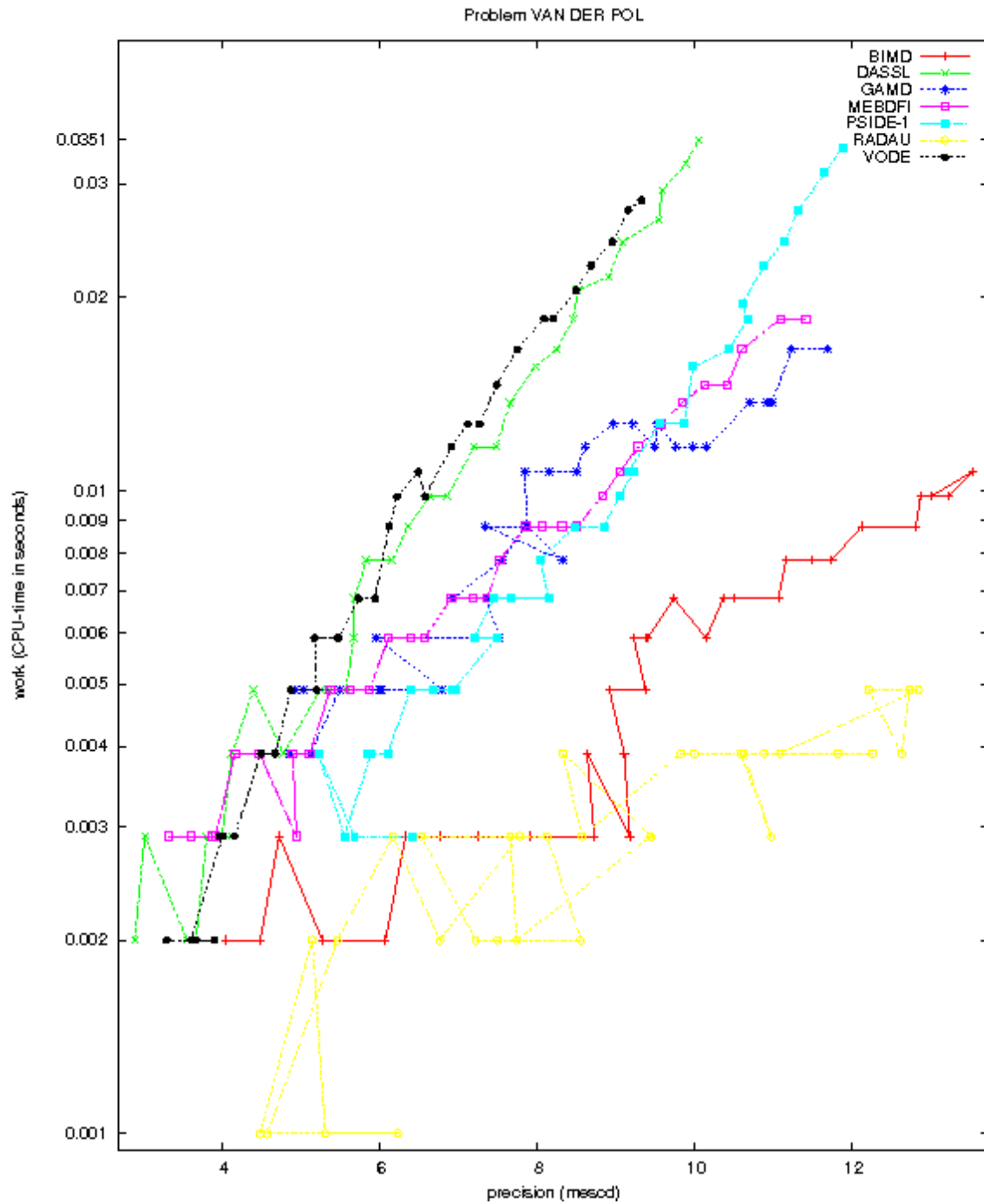


FIGURE II.8.8: Work-precision diagram (*mescd* versus CPU-time).

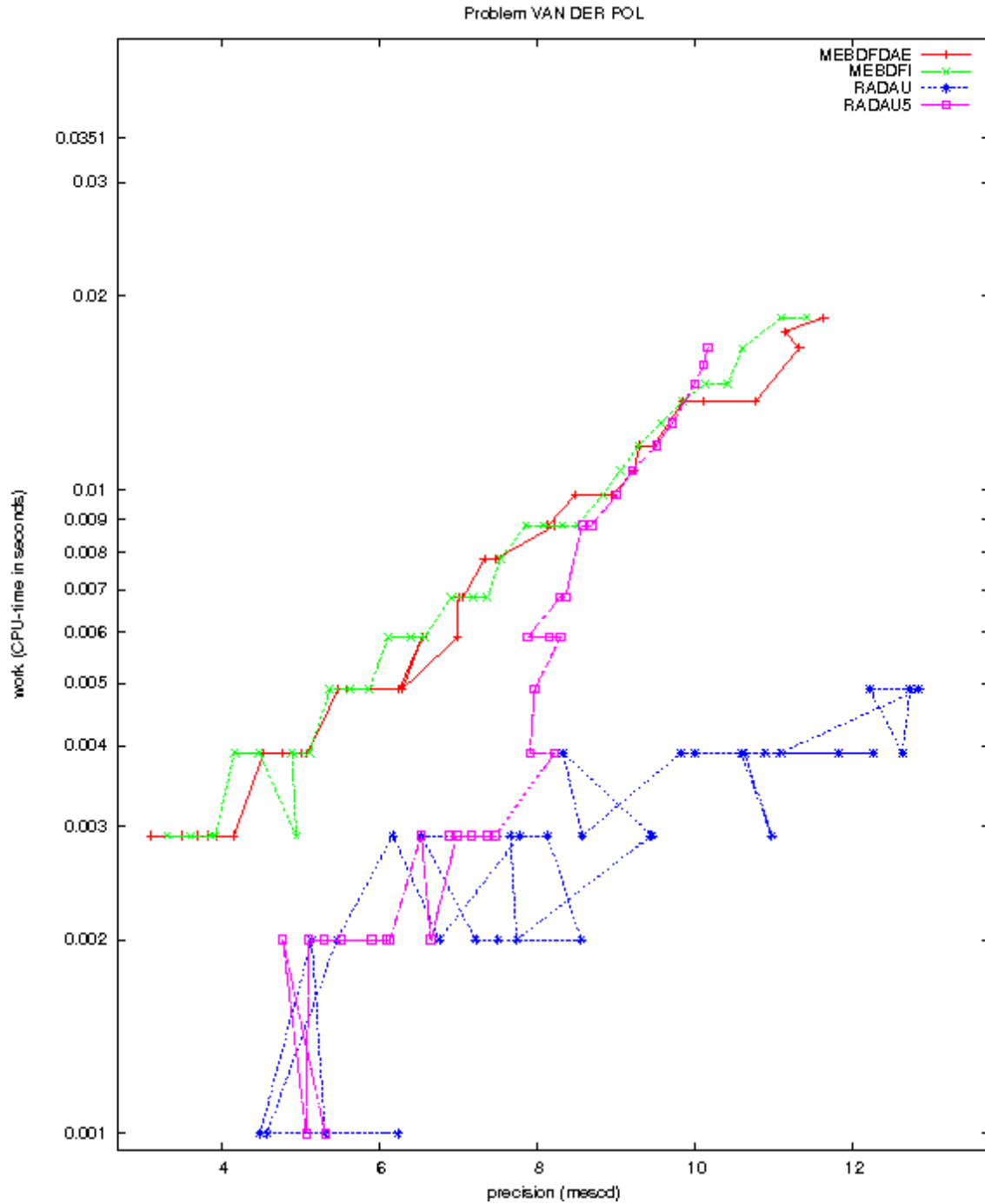


FIGURE II.8.9: Work-precision diagram (*mescd* versus CPU-time).

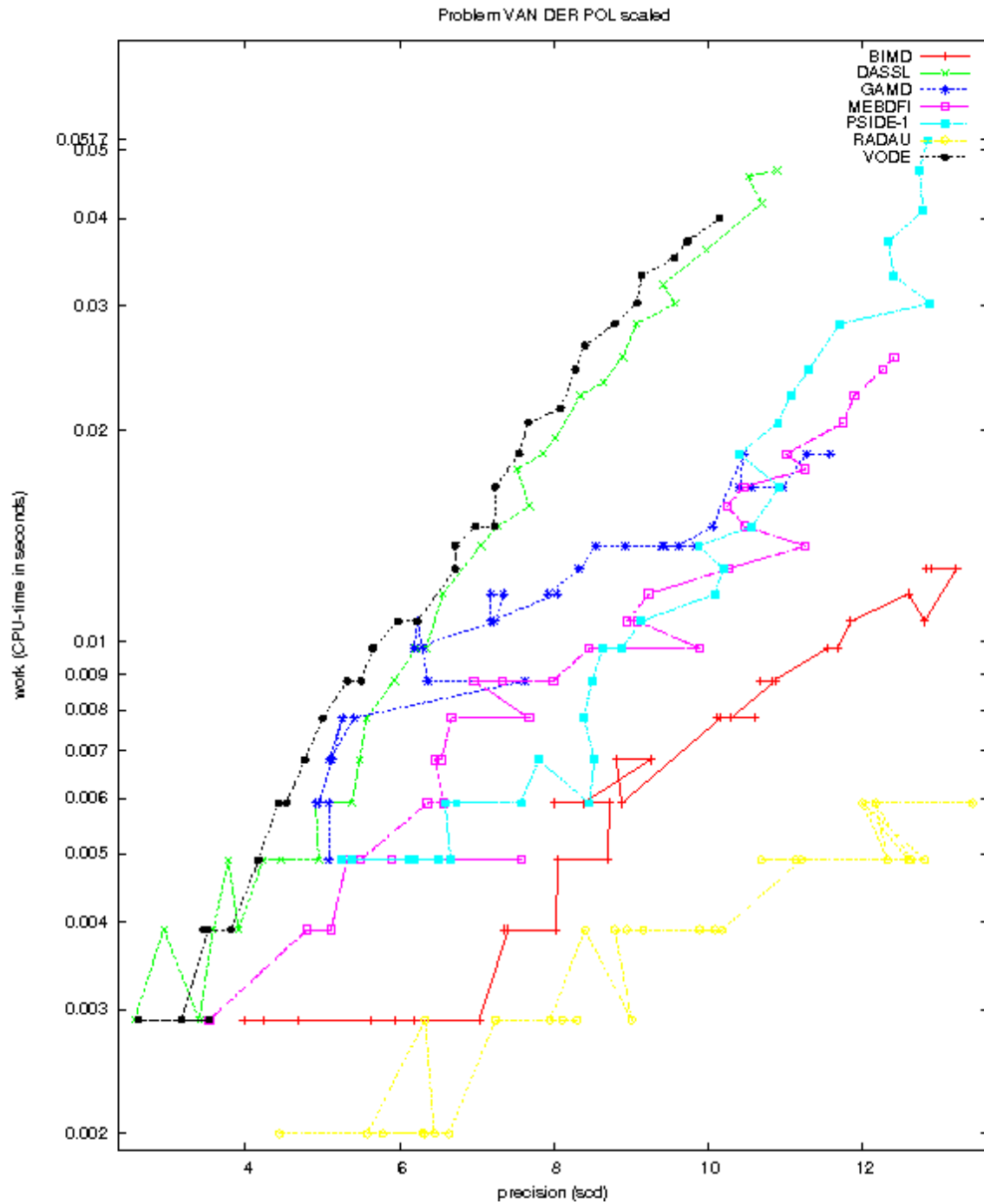


FIGURE II.8.10: Work-precision diagram (scd versus CPU-time).

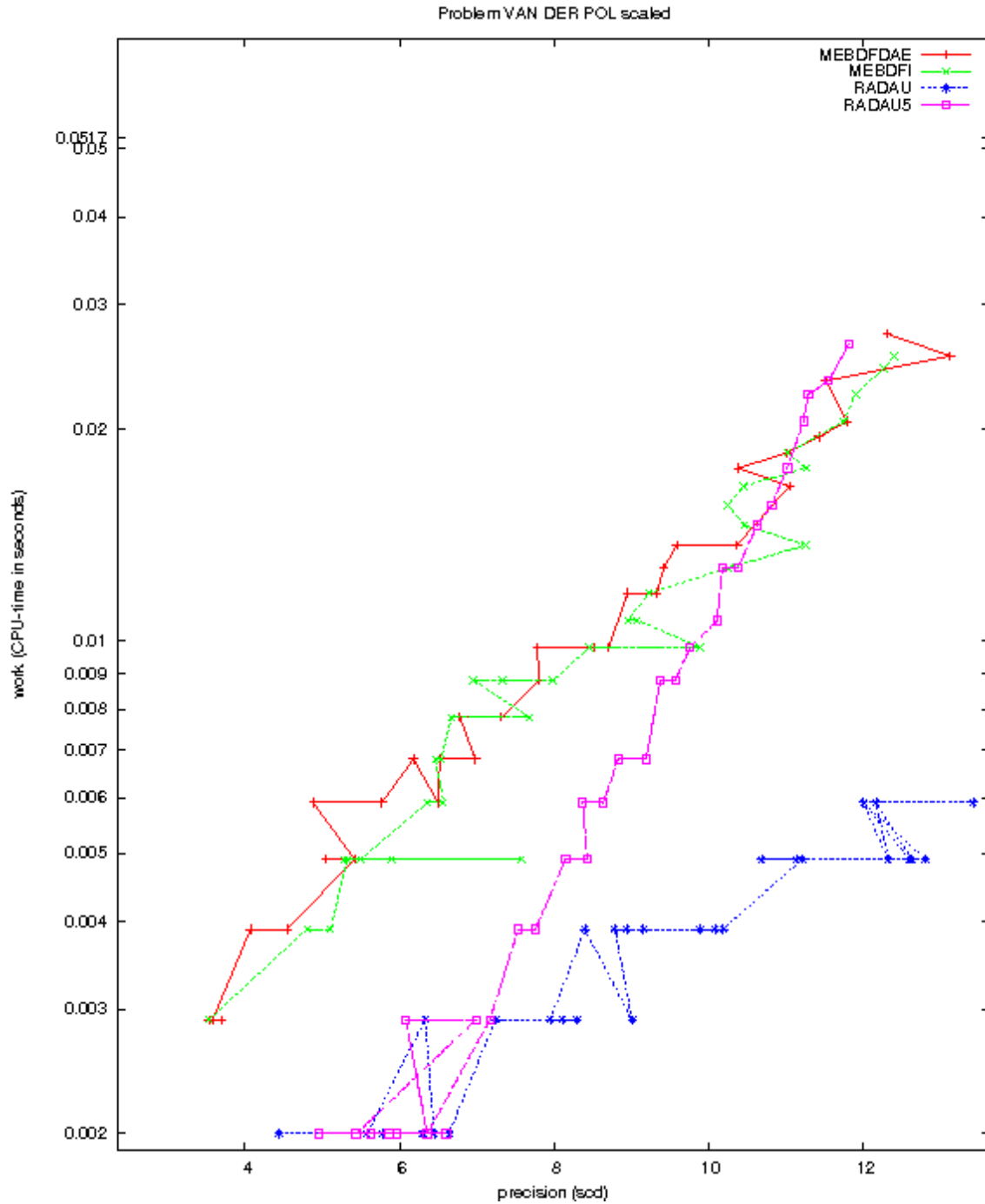


FIGURE II.8.11: Work-precision diagram (scd versus CPU-time).



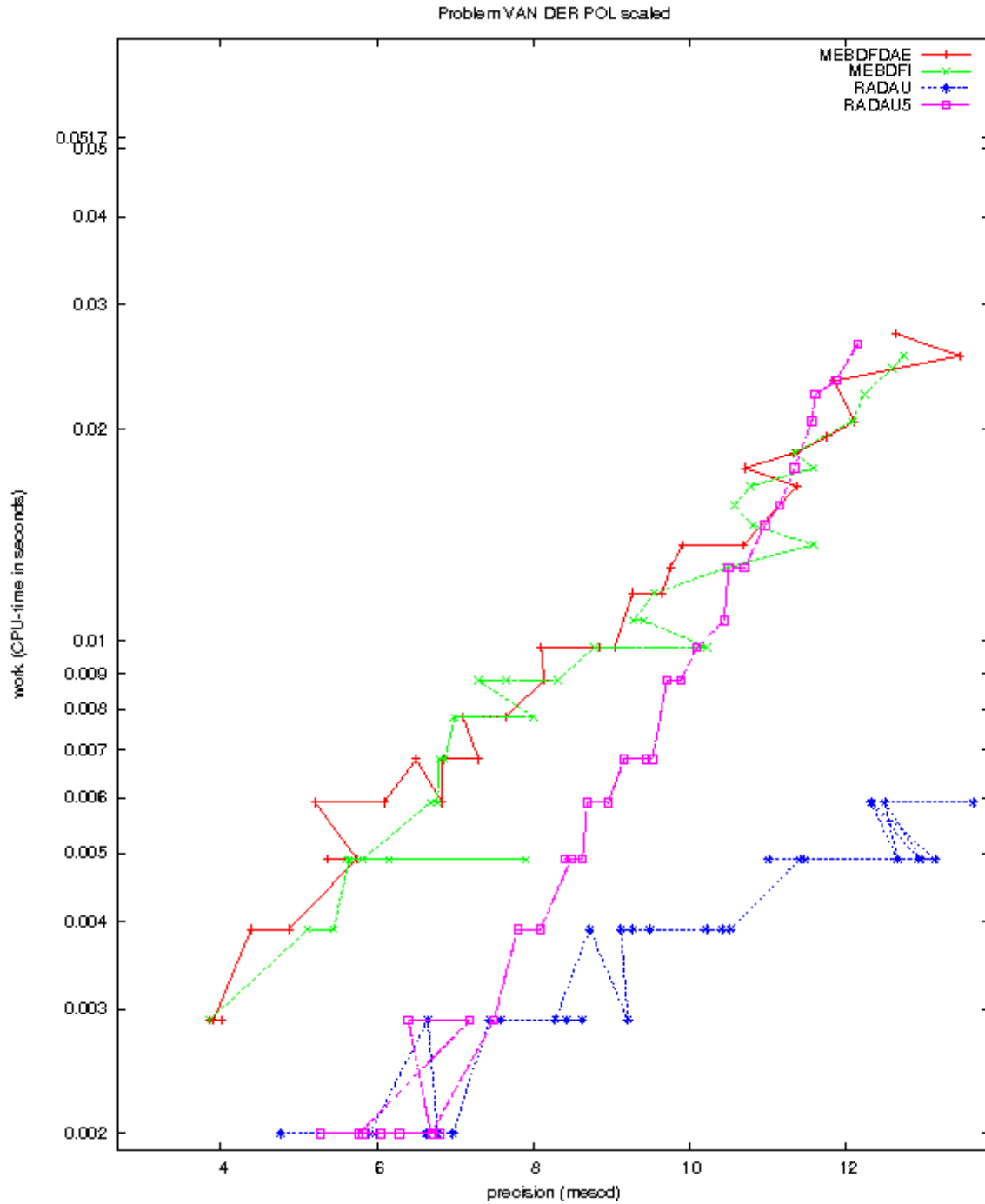


FIGURE II.8.13: Work-precision diagram (mescd versus CPU-time).

van der Pol, Selected Scientific Papers, vol. I, North Holland Publ. Comp. Amsterdam, 1960.